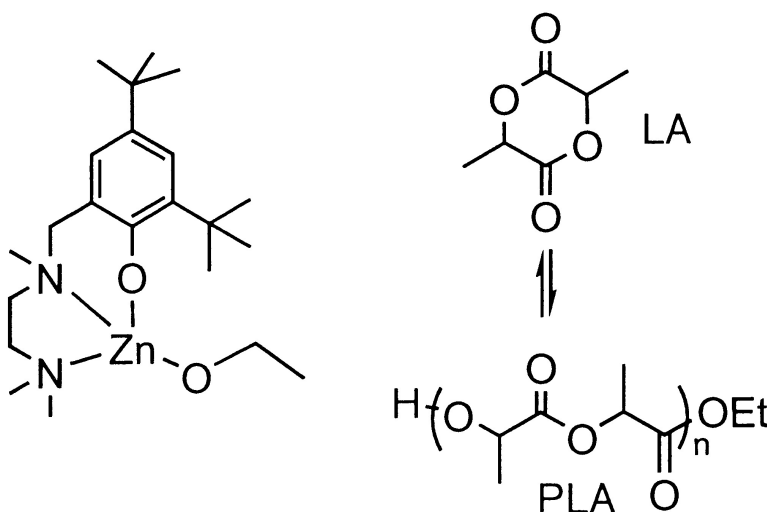Article

# A Highly Active Zinc Catalyst for the Controlled Polymerization of Lactide

Charlotte K. Williams, Laurie E. Breyfogle, Sun Kyung Choi, Wonwoo
Nam, Victor G. Young,, Marc A. Hillmyer, and William B. Tolman

## More About This Article

Additional resources and features associated with this article are available within the HTML version:

- Supporting Information
- Links to the 35 articles that cite this article, as of the time of this article download
- Access to high resolution figures
- Links to articles and content related to this article
- Copyright permission to reproduce figures and/or text from this article

View the Full Text HTML

# A Highly Active Zinc Catalyst for the Controlled Polymerization of Lactide

Charlotte K. Williams,[†] Laurie E. Breyfogle,[†] Sun Kyung Choi,[‡] Wonwoo Nam,[‡] Victor G. Young, Jr.,[†] Marc A. Hillmyer,*,[†] and William B. Tolman*,[†]

*Contribution from the Department of Chemistry, University of Minnesota, 207 Pleasant Street SE, Minneapolis, Minnesota, 55455 and Department of Chemistry and Division of Nano Sciences, Ewha Womans University, Seoul 120-750, Korea*

Received May 5, 2003;  E-mail: hillmyer@chem.umn.edu; tolman@chem.umn.edu

***Abstract:*** We report the preparation, structural characterization, and detailed lactide polymerization behavior of a new Zn(II) alkoxide complex, $(L_1ZnOEt)_2$ ($L_1$ = 2,4-di-*tert*-butyl-6-{[(2′-dimethylaminoethyl)methylamino]-methyl}phenolate). While an X-ray crystal structure revealed the complex to be dimeric in the solid state, nuclear magnetic resonance and mass spectrometric analyses showed that the monomeric form $L_1ZnOEt$ predominates in solution. The polymerization of lactide using this complex proceeded with good molecular weight control and gave relatively narrow molecular weight distribution polylactide, even at catalyst loadings of <0.1% that yielded $M_n$ as high as 130 kg $mol^{-1}$. The effect of impurities on the molecular weight of the product polymers was accounted for using a simple model. Detailed kinetic studies of the polymerization reaction enabled integral and nonintegral orders in $L_1ZnOEt$ to be distinguished and the empirical rate law to be elucidated, $-d[LA]/dt = k_p[L_1ZnOEt][LA]$. These studies also showed that $L_1ZnOEt$ polymerizes lactide at a rate faster than any other Zn-containing system reported previously. This work provides important mechanistic information pertaining to the polymerization of lactide and other cyclic esters by discrete metal alkoxide complexes.

## Introduction

The metal catalyzed ring-opening polymerization of lactide (LA), a renewable resource, is an efficient way to produce a biodegradable and recyclable plastic, polylactide (PLA).[1] The commercial production of PLA for applications in medicine, packaging, and fiber technology relies on this important catalytic transformation.[2] Diverse metal alkoxide complexes exhibit varying degrees of effectiveness for the polymerization of LA (and related cyclic esters), as reflected by differing rates and levels of polymerization control and stereoselectivity.[3] Notably lacking is fundamental mechanistic knowledge to help understand these differences and facilitate next-generation catalyst design. Thus, we aim to develop, structurally characterize, and carefully delineate the mechanistic behavior of new, discrete metal-alkoxide LA polymerization catalysts comprising nontoxic, inexpensive metals such as zinc[4] or iron.[5] In the case of Zn(II), simple salts suffer from low reactivity, limited solubility, and solution aggregation phenomena that complicate mechanistic

analysis (e.g., non first-order kinetic dependencies on catalyst concentration).[6,7] Alternatively, mononuclear "single-site" Zn(II) alkoxides supported by tris(pyrazolyl)hydroborate[8] or β-diketiminate[9,10] ligands, for example, have been shown to be quite active, controlled, and, in some cases,[11,12] stereoelective LA polymerization catalysts.

In a new strategy inspired by the cooperativity of dizinc sites in hydrolytic enzymes,[13] we recently reported the LA polymerization behavior for a dizinc complex of a dinucleating ligand HL.[4] For the purpose of comparison, we chose to examine a Zn(II) alkoxide supported by a closely related mononucleating



HL (R = tBu)  HL₁ (R = tBu)  HL₂ (R = Me)

---
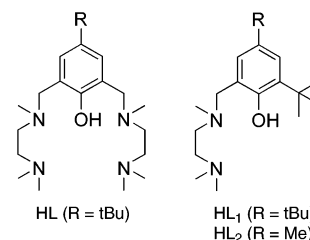
[†] University of Minnesota.
[‡] Ewha Womans University.

(1) (a) Drumright, R. W.; Gruber, P. R.; Henton, D. E. *Adv. Mater.* **2000**, *12*, 1841. (b) Amass, W.; Amass, A.; Tighe, B. *Polym. Int.* **1998**, *47*, 89.
(2) http://www.cdpoly.com/.
(3) (a) O'Keefe, B. J.; Hillmyer, M. A.; Tolman, W. B. *J. Chem. Soc., Dalton Trans.* **2001**, 2215. (b) Kuran, W. *Prog. Polym. Sci.* **1998**, *23*, 919. (c) Löfgren, A.; Albertsson, A.-C.; Dubois, P.; Jérôme, R. *J. Macromol. Sci., Rev. Macromol. Chem. Phys.* **1995**, *C35*, 379.
(4) Williams, C. K.; Brooks, N. R.; Hillmyer, M. A.; Tolman, W. B. *Chem. Commun.* **2002**, 2132.
(5) (a) O'Keefe, B. J.; Monnier, S. M.; Hillmyer, M. A.; Tolman, W. B. *J. Am. Chem. Soc.* **2001**, *123*, 339. (b) O'Keefe, B. J.; Breyfogle, L. E.; Hillmyer, M. A.; Tolman, W. B. *J. Am. Chem. Soc.* **2002**, *124*, 4384.

(6) (a) Noltes, J. G.; Verbeek, F.; Overmars, H. G. J.; Boersma, J. *J. Organomet. Chem.* **1970**, *24*, 257. (b) Nijenhuis, A. J.; Grijpma, D. W.; Pennings, A. J. *Polym. Bull.* **1991**, *26*, 71. (c) Barakat, I.; Dubois, Ph.; Jérôme, R.; Teyssie, Ph. *Macromolecules* **1991**, *24*, 6542. (d) Schwach, G.; Coudane, J.; Engel, R.; Vert, M. *Polym. Int.* **1998**, *46*, 177. (e) Kricheldorf, H. R.; Damrau, D. O. *Macromol. Chem. Phys.* **1998**, *199*, 1747.
(7) Kowalski, A.; Duda, A.; Penczek, S. *Macromolecules* **1998**, *31*, 2114 and references therein.
(8) Chisholm, M. H.; Eilerts, N. W.; Huffman, J. C.; Iyer, S. S.; Pacold, M.; Phomphrai, K. *J. Am. Chem. Soc.* **2000**, *122*, 11845.
(9) Chamberlain, B. M.; Cheng, M.; Moore, D. R.; Ovitt, T. M.; Lobkovsky, E. B.; Coates, G. W. *J. Am. Chem. Soc.* **2001**, *123*, 3229.
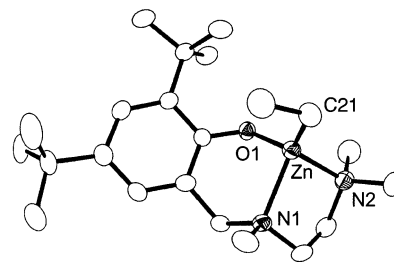
**Scheme 1**
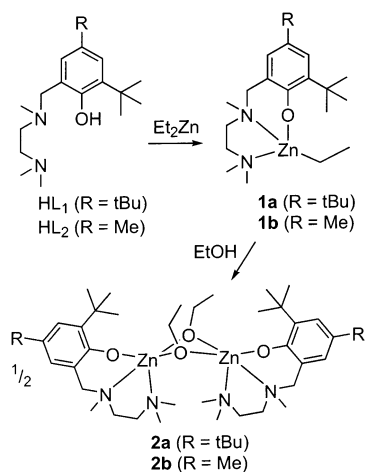


ligand (HL$_1$). We report herein the synthesis of such a complex and our finding that it polymerizes LA with good control and at a rate faster than any other Zn-containing system reported previously. Considerable effort has been expended to characterize the structure of the new complex, both in the solid state (X-ray crystallography, mass spectrometry) and in solution (NMR, pulsed gradient spin−echo (PGSE)[14]) under catalytically relevant conditions. Moreover, we disclose detailed studies of the polymerization reaction that elucidate the empirical rate law and provide important mechanistic information.

## Results

**Synthesis and Structures of Complexes.** The ligand HL$_1$ was prepared by refluxing *N,N,N′*-trimethylenediamine, *para*-formaldehyde, and 2,4-di-*tert*-butylphenol. A related ligand HL$_2$ (R = Me) was prepared in a similar manner and was used to synthesize an analogous complex to that made with HL$_1$ for crossover experiments (see below).[15] Reaction of HL$_1$ or HL$_2$ with Et$_2$Zn yielded rare examples of well-defined NNO-ligated zinc alkyls,[16] L$_1$ZnEt (**1a**) and L$_2$ZnEt (**1b**) (Scheme 1). The complexes were formulated on the basis of $^1$H and $^{13}$C{$^1$H} NMR spectroscopy, elemental analysis, and, for **1a**, an X-ray crystal structure (Figure 1, Table 1). The X-ray structure shows that **1a** is monomeric, with the four-coordinate Zn(II) ion adopting a distorted tetrahedral geometry. The differences between the angles C21−Zn−O1 (128.77(14)°) and N1−Zn−N2 (84.85(13)°) are illustrative of the distortion from an ideal tetrahedral topology. The Zn−C21 distance of 1.997(4) Å is slightly longer than usually seen for Zn(II)−alkyl bonds (1.93−1.98 Å).[16,17]

Treatment of these complexes with EtOH (∼1.2 equiv) generated the ethoxide complexes [L$_1$ZnOEt]$_n$ (**2a**) and [L$_2$-

(10) Chisholm, M. H.; Gallucci, J.; Phomprai, K. *Inorg. Chem.* **2002**, *41*, 2785.
(11) Coates, G. W. *J. Chem. Soc., Dalton Trans.* **2002**, 467.
(12) (a) Cheng, M.; Attygalle, A. B.; Lobkovsky, E. B.; Coates, G. W. *J. Am. Chem. Soc.* **1999**, *121*, 11583. (b) Ovitt, T. M.; Coates, G. W. *J. Am. Chem. Soc.* **1999**, *121*, 4072. (c) Ovitt, T. M.; Coates, G. W. *J. Polym. Sci., Part A: Polym. Chem.* **2000**, *38*, 4686.
(13) Selected reviews: (a) Sträter, N.; Lipscomb, W. N.; Klabunde, T.; Krebs, B. *Angew. Chem., Int. Ed. Engl.* **1996**, *35*, 2024. (b) Wilcox, D. E. *Chem. Rev.* **1996**, *96*, 2435. (c) Cowan, J. A. *Chem. Rev.* **1998**, *98*, 1067.
(14) Valentini, M.; Pregosin, P. S.; Rüegger, H. *Organometallics* **2000**, *19*, 2551.
(15) The polymerization activity of this complex was not explored.
(16) (a) Corey, E. J.; Yuen, P.-W.; Hannon, F. J.; Wierda, D. A. *J. Org. Chem.* **1990**, *55*, 784. (b) Dowling, C.; Parkin, G. *Polyhedron* **1996**, *15*, 2463. (c) Hammes, B. S.; Carrano, C. J. *Inorg. Chem.* **1999**, *38*, 4593.
(17) Looney, A.; Han, R.; Gorrell, I. B.; Cornebise, M.; Yoon, K.; Parkin, G.; Rheingold, A. L. *Organometallics* **1995**, *14*, 274.

**Figure 1.** Representation of the X-ray crystal structure of **1a**, with selected nonhydrogen atoms labeled and hydrogen atoms omitted for clarity. Selected bond distances (Å) and angles (deg): Zn1−O1, 1.956(2); Zn1−C21, 1.997(4); Zn1−N2, 2.128(3); Zn1−N1, 2.147(3); O1−Zn1−C21, 128.77(14); O1−Zn1−N2, 99.76(12); C21−Zn1−N2, 121.23(15); O1−Zn1−N1, 93.32(12); C21−Zn1−N1, 117.82(16); N2−Zn1−N1, 84.85(13).

**Table 1.** Summary of X-ray Crystallography Data

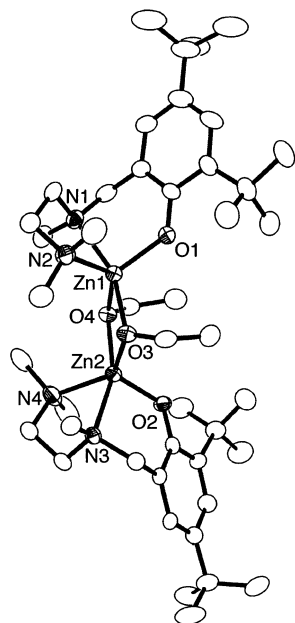|  | 1a | 2a |
|---|---|---|
| empirical foumula | C$_{22}$H$_{40}$N$_2$OZn | C$_{44}$H$_{80}$N$_4$O$_4$Zn$_2$ |
| formula weight | 413.93 | 859.86 |
| crystal system | monoclinic | orthorhombic |
| space group | P2$_1$/c | Pbcn |
| a (Å) | 11.9224(16) | 38.339(3) |
| b (Å) | 12.0853(16) | 17.0503(15) |
| c (Å) | 16.687(2) | 17.3185(15) |
| α (deg) | 90 | 90 |
| β (deg) | 103.489(2) | 90 |
| γ (deg) | 90 | 90 |
| V (Å$^3$) | 2338.1(5) | 11321.0(17) |
| Z | 4 | 8 |
| density (calcd) (g cm$^{-3}$) | 1.176 | 1.009 |
| crystal color and morphology | colorless, plate | colorless, plate |
| crystal size (mm$^3$) | 0.22 × 0.19 × 0.08 | 0.20 × 0.20 × 0.06 |
| absorption coefficient (mm$^{-1}$) | 1.062 | 0.882 |
| 2$\theta_{max}$ (deg) | 50.06 | 50.06 |
| no. of reflcns collected | 16067 | 30924 |
| no. of ind reflcns | 4121 | 9979 |
| no. of obsd reflcns [$I > 2\sigma(I)$] | 2894 | 6142 |
| parameters | 262 | 485 |
| R1$^a$ [$I > 2\sigma(I)$] | 0.0467 | 0.0514 |
| wR2$^b$ | 0.1233 | 0.1318 |
| goodness-of-fit | 0.990 | 0.947 |
| largest diff peak, hole (eÅ$^{-3}$) | 1.796, −0.472 | 0.461, −0.458 |

$^a$ R1 = $\Sigma||F_o| - |F_c||/\Sigma|F_o|$. $^b$ wR2 = $[\Sigma[w(F_o^2 - F_c^2)^2]/[\Sigma[w(F_o^2)^2]]^{1/2}$, where $w = 1/\sigma^2(F_o^2) + (aP)^2 + bP$.

ZnOEt]$_n$ (**2b**), which were isolated as colorless solids in >80% yield. The X-ray crystal structure of **2a** (Figure 2, Table 1) shows that in the solid state the complex exists as a dimer bridged by two ethoxides, the intermetal separation being 3.0835(6) Å. Each zinc atom is pentacoordinate with a distorted square pyramidal geometry.[18] The bridging oxygen atoms are asymmetrically placed between the two zinc atoms (e.g., O3 is 0.036 Å closer to Zn1 than to Zn2), as was also found for the dizinc complex of HL.[4]

The $^1$H NMR spectra of **1a**, **1b**, **2a**, and **2b** in CD$_2$Cl$_2$ contain single sets of sharp peaks at ambient temperature that are consistent with structures in solution that are monomeric, dimeric, or rapidly equilibrating mixtures. A representative spectrum of **2a** is shown in Figure S1 (Supporting Information). The features in this spectrum broaden and become more complex at low temperatures, indicating that a fluxional process-(es) is(are) operative. This process(es) could not be slowed sufficiently for study, even at −90 °C, so we have been unable to discern by simple variable temperature NMR spectral analysis whether intramolecular rearrangements or monomer/dimer equilibration (or both) are involved. Because the nuclearity of

(18) $\tau = 0.43$ for Zn(1), with O(1) axial, and $\tau = 0.40$ for Zn(2), with O(2) axial. See: Addison, A. W.; Rao, T. N.; Reedjik, J.; von Rijn, J.; Verschoor, G. C. *J. Chem. Soc., Dalton Trans.* **1984**, 1349.
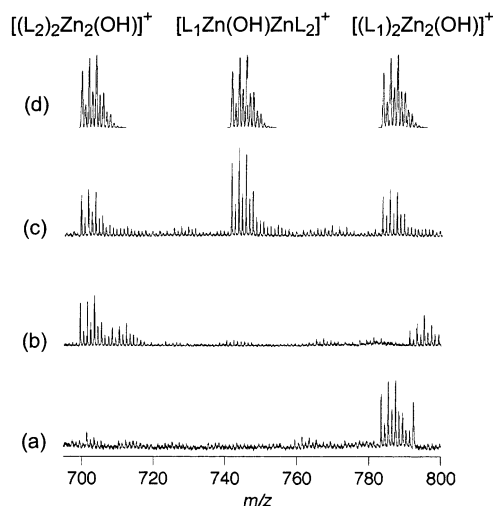
**Figure 2.** Representation of the X-ray crystal structure of **2a**, with selected nonhydrogen atoms labeled and hydrogen atoms omitted for clarity. Selected bond distances (Å): Zn1−Zn2, 3.0835(6); Zn1−O1, 1.945(3); Zn1−O3, 2.037(2); Zn1−O4, 2.009(2); Zn1−N1, 2.214(3); Zn1−N2, 2.268(3); Zn2−O2, 1.942(2); Zn2−O3, 2.001(2); Zn2−O4, 2.041(3); Zn2−N3, 2.233(3); Zn2−N4, 2.266(3).

**2a** in solution is of particular importance for understanding its catalytic behavior (see below), we performed additional experiments aimed specifically at determining whether **2a**, which by X-ray crystallography is dimeric with five-coordinate Zn(II) centers in the solid state, remains dimeric or cleaves into four-coordinate monomers in solution.

First, we performed crossover experiments whereby **2a** and **2b** were mixed in CH₂Cl₂ or CD₂Cl₂. Analysis of ¹H NMR spectra of mixtures with 2:1, 1:1, and 1:2 molar ratios of **2a** and **2b** in CD₂Cl₂ showed peaks identical to those of the independent complexes, with relative intensities that corresponded to their molar ratios. Although these data are consistent with **2a** and **2b** existing as monomers, as dimers or as either or both in rapid equilibrium, the absence of additional resonances rules out the exclusive formation of a heterodimeric species such as [L₁Zn(μ-OEt)₂ZnL₂] (unless such a species has NMR properties fortuitously identical to those of the separate compounds **2a** and **2b**).

To assess the possible equilibration between monomeric and dimeric structures, the solvent was removed from CH₂Cl₂ solutions of **2a**, **2b**, and mixtures of the two, and the resulting solids were analyzed by laser desorption mass spectrometry (LDMS). While parent ion envelopes were not observed for the separate complexes **2a** and **2b**, each exhibited a peak envelope corresponding to the respective dimeric ion [(L₁)₂Zn₂(OH)]⁺ and [(L₂)₂Zn₂(OH)]⁺ (Figure 3a and b), corroborated by spectral simulation (Figure 3d).[19] Laser ablation of the solid resulting from removal of CH₂Cl₂ from a 1:1 solution mixture of **2a** and **2b** after 30 min of equilibration time yielded the mass spectrum in Figure 3c. In addition to the same peaks as those seen for the separate samples of **2a** and **2b**, a new peak envelope appears at m/z ≈ 745 that corresponds to [L₁Zn(OH)ZnL₂]⁺. The approx-

(19) Rockwood, A. L.; VanOrden, S. L.; Smith, R. D. *Anal. Chem.* **1995**, *67*, 2699.

$[(L_2)_2Zn_2(OH)]^+$     $[L_1Zn(OH)ZnL_2]^+$     $[(L_1)_2Zn_2(OH)]^+$



**Figure 3.** LDMS data obtained on the solids resulting from evaporation of CH₂Cl₂ solutions of (a) **2a**, (b) **2b**, and (c) a 1:1 mixture of **2a** and **2b**. Simulations of the indicated ions are shown in part d.
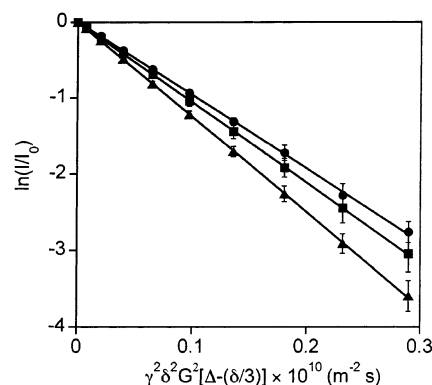


**Figure 4.** Plot of $\ln(I/I_0)$ vs $\gamma^2\delta^2G^2[\Delta-(\delta/3)] \times 10^9$ (m⁻² s) from PGSE experiments for **1a** (▲), **2a** (■), and **3** (●). The slopes (*D*) of the indicated linear fits were used to calculate *r* values (Table 2) as described in the text.

imate 1:2:1 intensity ratio of the three signals corresponding to the homo- and heterodimeric ions is consistent with the generation of monomers in solution that statistically dimerize in the solid state.

The question of whether **2a** exists primarily in solution as a monomer or dimer was also addressed through pulsed gradient spin−echo (PGSE) NMR measurements. The PGSE method assesses translational motion of the analyte in solution through determination of the diffusion coefficient, a quantity inversely related to its effective hydrodynamic volume.[20] The method has been used successfully for characterizing various organometallic systems,[14] including ones involved in monomer/dimer equilibria.[21] In addition to performing PGSE experiments on CD₂Cl₂ solutions of **2a**, we examined two reference compounds. These are **1a**, which is similar in size to the monomeric form of **2a**, and a larger Al complex [L"Al(OiPr)] (**3**) prepared in a separate work.[22] The results are displayed in Figure 4, plotted as $\ln(I/I_0)$ (where *I* = observed spin−echo intensity and $I_0$ = intensity in

(20) Price, W. S. *Concepts Magn. Reson.* **1997**, *9*, 299.
(21) (a) Geldbach, T. J.; Pregosin, P. S.; Albinati, A.; Rominger, F. *Organometallics*, **2001**, *20*, 1932. (b) Pichota, A.; Pregosin, P. S.; Valentini, M.; Wörle, M.; Seebach, D. *Angew. Chem., Int. Ed.* **2000**, *39*, 153. (c) Jiang, Q.; Rüegger, H.; Venanzi, L. M. *Inorg. Chim. Acta* **1999**, *290*, 64.
(22) L" = *N,N*-bis[methyl(2-hydroxy-3,5-di-*tert*-butylphenyl)]-*N′,N′*-dimethyl-ethylenediamine. Alcazar-Roman, L. M.; O'Keefe, B.; Hillmyer, M. A.; Tolman, W. B. *J. Chem. Soc., Dalton Trans.* **2003**, 3082.

**Table 2.** PGSE Experimental Results Compared to Estimated Data from X-ray Crystal Structures[a]

| complex | $D^b$ ($\times 10^{-10}$ m² s⁻¹) | $r^c$ (Å) | $a^d$ (Å) | $b^d$ (Å) | $r'^e$ (Å) | $D'$ ($\times 10^{-10}$ m² s⁻¹) |
|---|---|---|---|---|---|---|
| L₁ZnEt (**1a**) | 12.49(1) | 4.2(3) | 5.6(4) | 4.2(4) | 4.6(4) | 11.4(2) |
| [L"Al(OiPr)] (**3**) | 9.650(9) | 5.4(3) | 6.8(5) | 5.5(4) | 5.9(5) | 9.0(2) |
| **2a** | 10.55(2) | 4.9(3) | 9.9(7) | 5.6(4) | 6.8(6) | 7.6(2) |

[a] Estimated errors are indicated in parentheses, with terms defined in the text. [b] From slopes of the lines in Figure 4, eq 1, and eq 2. [c] The errors are estimated to be ~5% primarily on the basis of the accuracy of $\eta$ used in the calculation. [d] Estimated values from the X-ray crystal structure by measuring the lengths between the centers of distant hydrogen atoms on the periphery corresponding to each arbitrary axis and by calculating the minimum ellipsoid into which the molecule fits. [e] Calculated using eq 3.

the absence of gradients), versus a function with the square of the gradient strength over a constant diffusion time. Each data point represents an average of the values obtained for the different resonances in the NMR spectrum of each compound at varying gradient strengths. The slopes of the lines in Figure 4 are equal to the diffusion coefficients ($D$) according to eq 1 (where $G$ = gradient strength, $\gamma$ = gyromagnetic ratio, $\delta$ = length of gradient pulse, and $\Delta$ = delay between gradient midpoints). The absolute value of the slope decreases with increasing effective hydrodynamic radii according to the Stokes–Einstein equation (eq 2, where $r$ = effective hydrodynamic radius and $\eta$ = viscosity). The experimentally determined values of $D$ and $r$ were calculated and are listed in Table 2. From these data for solutions of the three complexes analyzed, the following ranking of effective hydrodynamic volumes is given: **3** > **2a** > **1a**.

For comparison, we estimated values of the molecular radii ($r'$) for **1a**, **2a**, and **3** from their X-ray crystal structures by measuring the lengths between centers of distant hydrogen atoms on the molecular periphery.[23] All of the complexes were considered as prolate ellipsoids with major and minor axes $a$ and $b$, respectively (Table 2), and $r'$ was determined by using eq 3.[24] Importantly, the values of $r$ (PGSE) and $r'$ (X-ray) for **1a** and **3** closely agree. In contrast, for **2a**, the radius determined by the PGSE measurement ($r$) is ca. 25% smaller than the radius estimated from the X-ray crystal structure ($r'$) of the dinuclear form. These data strongly suggest that **2a** does not retain its dimeric form in solution.

We also calculated diffusion coefficients ($D'$) from the values of $a$, $b$, and $r'$, which required the use of a variant of eq 2 appropriate for prolate ellipsoids.[24] As expected, the agreement between the PGSE measured ($D$) and predicted ($D'$) diffusion coefficients is excellent for **1a** and **3** (consistent with the agreement of $r$ and $r'$), but $D'$ for **2a** is much less than the measured value, again consistent with the form of **2a** in solution being significantly smaller than the dinuclear structure adopted in the crystal. On this basis, therefore, we postulate that **2a** exists predominantly as a monomer in CD₂Cl₂. As a check on this hypothesis, we estimated an upper bound for the radius expected for monomeric L₁ZnOEt, $r'$ = 5.3 Å, by adding approximately one-half of the distance of an O–Et bond (0.7 Å) to the $r'$ value

(23) Hydrodynamic volumes may be estimated via an alternative method of PGSE data analysis that uses summations of van der Waals radii, but this method was not utilized for the complexes studied herein because of possible inaccuracies resulting from void spaces in the structures. Stahl, N. G.; Zuccaccia, C.; Jensen, T. R.; Marks, T. J. *J. Am. Chem. Soc.* **2003**, *125*, 5256.

(24) Price, W. S. In *New Advances in Analytical Chemistry*; Rahman, A.-ur-. Ed.; Hardwood Academic Publishers: Singapore, 2000; pp 31–72.

**Table 3.** Representative Results for the Polymerization of LA by **2a**[a]

| [LA]₀/[L₁ZnOEt]₀ | time (min) | conversion (%)[b] | $M_n$ (kg mol⁻¹)[c] | PDI[c] |
|---|---|---|---|---|
| 650 | 5 | 96 | 67 | 1.42 |
| 1000 | 13 | 96 | 99 | 1.40 |
| 1500 | 18 | 93 | 130 | 1.34 |

[a] Conditions: CH₂Cl₂, 25 °C, [LA]₀ = 1 M, in a glovebox. [b] Determined by ¹H NMR spectroscopy. [c] Determined by SEC using light scattering detection (see Experimental Section).

for **1a** (4.6 Å). This estimated $r'$ was then used to calculate $D'$ = 10.0 × 10⁻¹⁰ m² s⁻¹ (assuming a spherical shape for the molecule). Both the estimated $r'$ and $D'$ values for the putative monomeric form of L₁ZnOEt closely agree with those that were experimentally determined for **2a**, consistent with assignment of the monomeric structure L₁ZnOEt in solution. As such, we refer to **2a** in solution as L₁ZnOEt in the following discussion of its polymerization behavior.

$$\ln\left(\frac{I}{I_0}\right) = -\gamma^2\delta^2G^2\left(\Delta - \frac{\delta}{3}\right)D \qquad (1)$$

$$D = \frac{kT}{6\pi\eta r} \qquad (2)$$

$$r' = (ab^2)^{1/3} \qquad (3)$$

**Polymerization Activity.** While **1a** does not polymerize D,L-LA, consistent with a coordination insertion mechanism requiring an initiating and propagating metal alkoxide,[25] **2a** is highly active for the polymerization of D,L-LA in CH₂Cl₂ at ambient temperature (Table 3). Polymerizations were performed under strictly dry and anaerobic conditions in a glovebox with initial monomer concentrations, [LA]₀, of 1 M. Conversions were assayed by ¹H NMR spectroscopy, and accurate polymer molecular weights and polydispersities were determined in all cases by size exclusion chromatography (SEC) using multi-wavelength light scattering detection. We observed rapid reactions over a wide range of initial monomer-to-catalyst ratios, with a high conversion of LA possible even up to [LA]₀/[L₁ZnOEt]₀ ratios of 1500, yielding PLA with molecular weights as large as 130 kg mol⁻¹. We have found no other report of a Zn(II) complex that is effective at such low levels of catalyst loading ([L₁ZnOEt]₀ ≈ 0.7 mM). Good molecular weight control is demonstrated by a linear increase in $M_n$ with LA conversion at [LA]₀/[L₁ZnOEt]₀ = 1000 (Figure 5) and relatively narrow molecular weight distributions of the products (polydispersity index, PDI ≈ 1.4). Despite the linear dependence of $M_n$ with LA conversion, the polylactide molecular weights are lower than expected (dotted line in Figure 5) based on the initial concentrations of catalyst and monomer, particularly at high conversion. These features also are evident in a plot of $M_n$ versus ([LA]₀ − [LA]ₜ)/[L₁ZnOEt]₀, measured over a wide range of initial monomer-to-catalyst ratios (filled circles, Figure 6). For example, at [LA]₀/[L₁ZnOEt]₀ = 1500 at 98.5% conversion, the PLA molecular weight should be 214 kg mol⁻¹ compared to the experimental value of 130 kg mol⁻¹.

Such divergences from anticipated molecular weights may be explained by an effective concentration of catalyst, [L₁-

(25) Duda, A.; Penczek, S. *Polymers from Renewable Resources: Biopolyesters and Biocatalysis*; Scholz, C., Gross, R. A., Eds.; ACS Symposium Series Vol. 764; American Chemical Society: Washington, DC, 2000; pp 160–198.
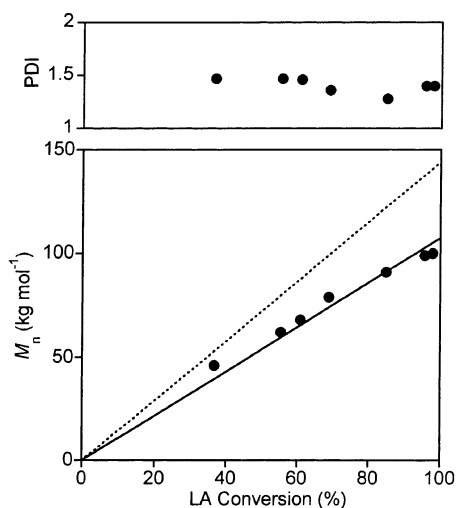
**Figure 5.** Plot of $M_n$ and PDI vs conversion for the polymerization of LA by **2a**. Conditions: $[LA]_0 = 1$ M, $[LA]_0/[L_1ZnOEt]_0 = 1000$, $CH_2Cl_2$, 25 °C. The dashed line represents the expected relationship of $M_n$ with % conversion based on eq 4 with $C = 0$ mM, while the solid line is the fit of the data to eq 4, yielding $C = 0.34(3)$ mM.
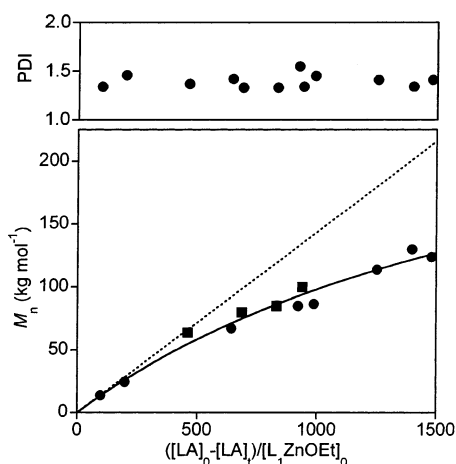


**Figure 6.** Plot of $M_n$ (● in the absence of added BnOH, ■ with added BnOH) and PDI vs $([LA]_0 - [LA]_t)/[L_1ZnOEt]_0$ for the polymerization of LA by **2a**. All LA conversions were $> 83\%$. Conditions: $[LA]_0 = 1$ M, $CH_2Cl_2$, 25 °C. For the points corresponding to runs with added BnOH (■), $[L_1ZnOEt]_0 = 0.67$ mM $+ [BnOH]_0$. The dashed line represents the expected relationship of $M_n$ with $([LA]_0 - [LA]_t)/[L_1ZnOEt]_0$ based on eq 4 with $C = 0$ mM, while the solid curve is the fit of the data to eq 4, yielding $C = 0.46(3)$ mM.

ZnOEt]$_{eff}$, that differs from the amount added, $[L_1ZnOEt]_0$, due to the presence of impurities that may destroy some of the catalyst (catalyst deactivator, CD) and/or promote rapid exchange between a propagating chain and an exchange agent (EA)[26] or a polymeric alcohol. An EA would cause $[L_1ZnOEt]_{eff}$ to be greater than $[L_1ZnOEt]_0$, increase the total number of polymer chains, and thus decrease $M_n$ at a fixed conversion, while a CD would have the opposite effect. These relationships are described by eq 4, where $C = [EA] - [CD]$. This analysis reasonably assumes that chain exchange equilibria are more rapid than propagation.[27] A fit of the data in Figure 5 to eq 4 (where $[LA]_0 - [LA]_t = \%$ conversion/100; $[LA]_0 = 1$ M) is shown as the solid line and yields $[L_1ZnOEt]_{eff} = 1.34(3)$ mM.

(26) Odian, G. *Principles of Polymerization*; John Wiley & Sons: New York, 1991; pp 538−540.
(27) Ovitt, T. M.; Coates, G. W. *J. Polym. Sci., Part A: Polym. Chem.* **2000**, *38*, 4686.

Accordingly, since [CD] can conceivably range from 0 (no deactivating impurity) to just less than 1 mM ($= [L_1ZnOEt]_0$, thus virtually all catalyst destroyed), the range of possible values for [EA] in this analysis is 0.34 mM $<$ [EA] $<$ 1.34 mM.

$$M_n = \frac{([LA]_0 - [LA]_t)(144 \text{ g mol}^{-1})}{[L_1ZnOEt]_0 + C} \qquad (4)$$

To further test the feasibility of rapid chain exchange during catalysis by **2a**, we added various amounts of benzyl alcohol (BnOH) to polymerization reactions performed with a low concentration of catalyst ($[L_1ZnOEt]_0 \approx 0.7$ mM, $[LA]_0 = 1$ M). No significant changes in the rate of PLA production or the polylactide PDI with added BnOH were obvious, indicating that **2a** retains its activity in the presence of added alcohol (even at $[ROH]_0/[L_1ZnOEt]_0 = 150$, for R = Et). Importantly, added BnOH caused $M_n$ to decrease, as shown by the data plotted as squares in Figure 6 (for these points, we used $[L_1ZnOEt]_0 = 0.67$ mM $+ [BnOH]_0$, where $[BnOH]_0 = 0.17-1.34$ mM). As predicted for BnOH acting as a rapid EA, the data (squares) closely parallel those obtained when $([LA]_0 - [LA]_t)/[L_1ZnOEt]_0$ was varied in the absence of BnOH (circles). Indeed, in an analysis analogous to that applied to Figure 5, the combined data in Figure 6 may be fit (solid curve) to eq 4, where EA is now the "intrinsic" impurity present in the absence of added BnOH. The resulting value $C = 0.46(3)$ mM yields a range 0.46 mM $<$ [EA] $<$ 1.13 mM ($0 <$ [CD] $< 0.67$ mM), in satisfyingly close agreement with the results from the analysis of the independently acquired data in Figure 5. In sum, the results confirm that LA polymerizations by **2a** are sensitive to rapid chain exchange both by purposefully added BnOH and by an impurity EA. The amount of this EA has been estimated by considering possible limiting values of a CD, independent kinetic evidence for which is presented in the next section.

We determined that the ethoxide group of **2a** initiates the polymerization of LA through acyl cleavage by performing polymerizations at high catalyst loadings. A reaction performed with $[LA]_0/[L_1ZnOEt]_0 = 50$ was quenched after 10 s (95% conversion) and analyzed by ^{1}H NMR spectroscopy. Both ethoxy ester and hydroxy end groups were visible in the spectrum in a 1:1 ratio. However, by integration there were 70 LA units per endgroup, rather than 50 as predicted from the $[LA]_0/[L_1ZnOEt]_0$ ratio used. In addition, the PDI of the resulting polymer was broad (2.31). We hypothesize that the low level of ethoxy end groups and high PDI under these conditions (high catalyst loading) may be due to initiation being somewhat slower than propagation. In separate experiments using $[LA]_0/[L_1ZnOEt]_0 = 1075$ and 20 equiv of added EtOH exchange reagent, the discrepancy between experimental observations and theory narrowed. At 92% conversion, 49 LA units were expected per endgroup; 46 were observed via ^{1}H NMR integration. The combined data firmly establish that ethoxy groups initiate polymer chain growth, presumably through a coordinative insertion pathway.

Finally, ^{1}H NMR spectroscopic analysis of PLA produced from D,L-LA indicates an atactic microstructure, even when the polymerization was performed at low temperature (0 °C).[28] A

(28) Thakur, K. A. M.; Kean, R. T.; Hall, E. S.; Kolstad, J. J.; Munson, E. J. *Macromolecules* **1998**, *31*, 1487.

**Table 4.** Observed Rate Constants for LA Polymerization by **2a** Relative to Selected Complexes[a]

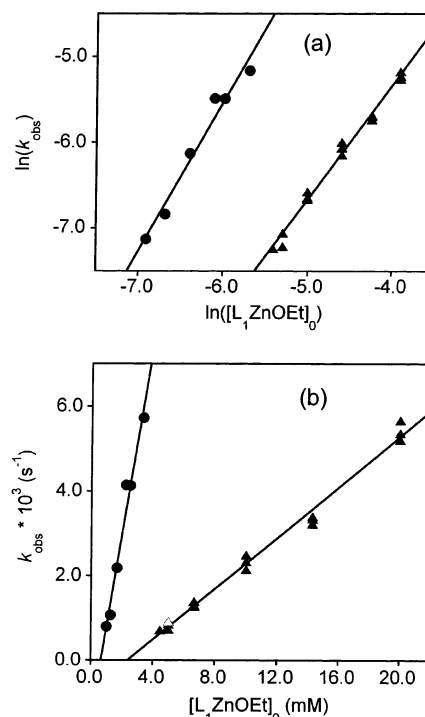| complex | $k_{rel}$[b] | [complex]$_0$ (mM) | ref |
|---|---|---|---|
| (BDI)ZnOiPr | 5.1 | 2.1 | 9 |
| LZn$_2$Cl$_2$OEt | 8.2 | 3.3 | 4 |
| TpMgOEt | 36 | 11 | 8 |
| TpZnOEt | 1220 | 11 | 8 |

[a] Conditions: $CH_2Cl_2$ or $CD_2Cl_2$ at 25 °C. [b] Equal to the ratio $k_{obs}(\mathbf{2a})$/$k_{obs}$(complex) at [complex]$_0$ = [L$_1$ZnOEt]$_0$. Values of $k_{obs}(\mathbf{2a})$ were calculated using $k_{obs}(\mathbf{2a}) = k_{prop}$[L$_1$ZnOEt]$_0$, with $k_p$ = 2.2 M$^{-1}$ s$^{-1}$.

sample of PLA derived from L-LA was isotactic, indicating no discernible epimerization during the polymerization.

**Polymerization Kinetics.** Insight into the mechanism of polymerization of LA by **2a** was obtained through kinetics studies. Polymerizations were performed at either of two temperatures at a fixed initial lactide concentration ([LA]$_0$ = 1.0 M at 25 °C or [LA]$_0$ = 0.5 M at 0 °C), and catalyst concentrations were varied over a range [L$_1$ZnOEt]$_0$ = 1−20 mM. The polymerizations were continually monitored via in situ FTIR spectroscopy (ReactIR). All polymerizations showed a first order dependency on the concentration of LA over at least four half-lives. The observed rate constants ($k_{obs}$) for each run were extracted from the exponential polymer growth/monomer decay curves (Figure S2, Table S1). At ambient temperature, the $t_{1/2}$ is ≈ 2.5 min for [L$_1$ZnOEt]$_0$ = 2.2 mM (0.2 mol % Zn relative to lactide). To draw comparisons to previously reported kinetic data for other catalysts, we list relative rate constants $k_{rel}$, defined as the ratio of $k_{obs}$ for L$_1$-ZnOEt vs $k_{obs}$ for each complex (at equivalent concentrations of complex) in Table 4.[4,8,9] The data show that **2a** is the fastest Zn-containing LA polymerization catalyst discovered.[29]

To determine the kinetic order in [Zn], we analyzed the dependence of $k_{obs}$ on [L$_1$ZnOEt]$_0$. Plots of ln($k_{obs}$) vs ln([L$_1$-ZnOEt]$_0$) are linear (Figure 7a), but with noninteger slopes of 1.33 (at 0 °C) and 1.75 (at 25 °C). The plots suggest the intriguing proportionality −d[LA]/d$t$ ∝ [L$_1$ZnOEt]$^n$ with $n$ = 1.33 (0 °C) or 1.75 (25 °C). Such noninteger orders in catalyst are difficult to interpret mechanistically, although models that incorporate complicated aggregation phenomena have been postulated for such cases.[9,30] In an alternative interpretation of the data, plots of $k_{obs}$ vs [L$_1$ZnOEt]$_0$ are linear, indicating a first order dependency of the rate on [L$_1$ZnOEt] (Figure 7b) and giving the rate law −d[LA]/d$t$ = $k_p$[L$_1$ZnOEt][LA], with $k_p$ = propagation rate constant = 2.2 M$^{-1}$ s$^{-1}$ at 25 °C and 0.30 M$^{-1}$ s$^{-1}$ at 0 °C. This rate law is consistent with a mechanism involving coordinative insertion at a single Zn site.

The $x$-intercepts for the linear fits shown in Figure 7b are nonzero, suggesting that there is a threshold catalyst concentration below which polymerization will not occur.[5] For the kinetic runs performed at 25 °C, the threshold value is 0.7 mM, but at 0 °C it is 2.4 mM. Note that the experimental procedures differed at the two temperatures; at 25 °C polymerization was initiated by adding the catalyst stock solution to a solution of LA in the glovebox and then removing the flask from the glovebox for monitoring by ReactIR, but at 0 °C it was necessary to perform

(29) While no detailed kinetic data are available for some recently reported highly active Ca[29a] and Mg[29b] catalysts, to a first approximation, **2a** is comparably effective. (a) Chisholm, M. H.; Gallucci, J.; Phomphrai, K. *Chem. Commun.* **2003**, 48. (b) Chisholm, M. H.; Huffman, J. C.; Phomphrai, K. *J. Chem. Soc., Dalton Trans.* **2001**, 222.
(30) Kowalski, A.; Libiszowski, J.; Duda, A.; Penczek, S. *Macromolecules* **2000**, *33*, 1964.



**Figure 7.** Kinetic plots for the polymerization of LA by **2a** at 25 °C (●) and 0 °C (▲). Conditions: $CH_2Cl_2$, [LA]$_0$ = 1.0 M (25 °C) or 0.5 M (0 °C). The open triangle in part b is the data point for the experiment (0 °C) in which [L$_1$ZnOEt]$_0$ was initially 1.0 mM (no polymerization) and then was increased to 5.0 mM (polymerization initiated); see text.

the entire procedure on the benchtop by addition of catalyst via syringe injection through a septum to a precooled LA solution immersed in an ice bath with the ReactIR probe inserted. Introduction of a trace impurity is more difficult to avoid in the latter case. The 25 °C threshold value also is essentially the same catalyst concentration used in successful batch polymerizations using [LA]$_0$/[L$_1$ZnOEt]$_0$ = 1500 (Table 3) that were kept in the glovebox for the entire reaction time. Taken together, these results imply that there is a low level of impurity relative to [LA]$_0$ = 1 M (or [LA]$_0$ = 0.5 M at 0 °C) that deactivates the catalyst and that the amount of impurity (CD) varies with experimental protocol, suggesting that it may be introduced inadvertently. Several additional experiments were performed to test these hypotheses.
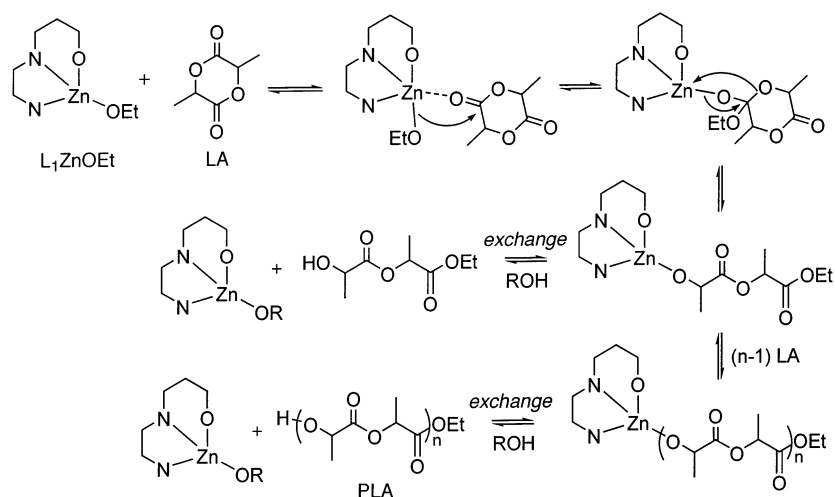
First, a kinetic experiment was run at 0 °C using syringe transfer conditions and a catalyst concentration below the threshold ([L$_1$ZnOEt]$_0$ = 1.0 mM). ReactIR monitoring showed polymerization neither after ∼30 min nor after warming to 25 °C and standing for an additional 30 min. These results show that slow initiation at 0 °C is not responsible for the absence of polymerization at low [L$_1$ZnOEt]$_0$ in the syringe transfer kinetic runs. In another kinetic experiment run under syringe transfer conditions at 0 °C using [L$_1$ZnOEt]$_0$ = 1.0 mM, monitoring for ∼1.5 h again showed no PLA production, but subsequent addition of **2a** to bring the total catalyst concentration to 5.0 mM (i.e., above the threshold) triggered the reaction. Polymerization proceeded with a $k_{obs}$ value of 9.2 × 10$^{-4}$ s$^{-1}$ (open triangle in Figure 7b), in line with values obtained in kinetic runs that began with this amount of catalyst. This result is consistent with the hypothesis of an impurity (CD) that prohibits polymerization catalysis when [L$_1$ZnOEt]$_0$ < 2.4 mM at 0 °C.

*Scheme 2*



Working under the notion that this impurity was introduced during the syringe transfer protocol necessary for ReactIR monitoring in the 0 °C kinetic runs, we modified the procedure to see if the impurity level could be lowered sufficiently to enable polymerization below the [CD] = 2.4 mM threshold at 0 °C. We carefully vacuum transferred $CH_2Cl_2$ onto a solid mixture of LA (1 M) and **2a** ([$L_1ZnOEt]_0$ = 2.0 mM) at −80 °C, warmed the mixture to 0 °C, and allowed the reaction to run for 2 h at 0 °C. PLA was formed to greater than 90% conversion, confirming that if appropriate care is taken, the impurity level can be reduced sufficiently to enable polymerization at low [$L_1ZnOEt]_0$ at 0 °C. Finally, SEC data for polymers from kinetic runs at both temperatures at equal [LA]$_0$/[$L_1ZnOEt]_0$ (=500) revealed different $M_n$ values: $M_n$ (0 °C) = 14.7 kg mol$^{-1}$ versus $M_n$ (25 °C) = 46.2 kg mol$^{-1}$. The finding of lower polymer molecular weight with higher levels of deactivating impurity suggests that the product of the catalyst deactivation is itself a chain exchange agent.

A candidate for the adventitious/introduced impurity is water, since addition of 1 equiv (relative to $L_1ZnOEt$) of water completely terminated a kinetic experiment at 25 °C. In a second experiment ([LA]$_0$/[$L_1ZnOEt]_0$ = 20), polymerization proceeded to >95% conversion upon addition of 0.5 equiv of water. A possible explanation for the effects of water on the polymerization reaction is presented below.

## Discussion

We have characterized a new Zn(II) alkoxide **2a** that exhibits good control in the polymerization of LA to yield high molecular weight PLA at rates faster than other Zn systems reported to date. Scheme 2 shows a proposed mechanism for the polymerization of LA catalyzed by **2a** consistent with the combined structural, reactivity, and kinetic data. Although dimeric in the solid state, as shown by X-ray crystallography and LDMS, the results of crossover experiments with analogue **2b** and, most convincingly, the PGSE data indicate that in $CH_2Cl_2$ solution at ambient temperature **2a** exists predominantly as a monomer. Since the LA polymerizations were performed under the same conditions (25 °C, $CH_2Cl_2$), we thus conclude that the resting and, most likely, the catalytically active form of **2a** is the monomeric species $L_1ZnOR$.

This conclusion is further supported by the results of the kinetics experiments, from which we deduce an overall second

order rate law, with first order dependencies on [LA] and on [$L_1ZnOR$] but with the presence of a low level (0.07−0.48% based on [LA]$_0$) of impurity that prohibits polymerization below a threshold catalyst concentration. In addition to being indicated by the nonzero intercepts in plots of $k_{obs}$ versus [$L_1ZnOEt]_0$ (Figure 7b), the presence of such an impurity was supported by several independent experiments, perhaps the most critical being commencement of polymerization upon addition of catalyst to a nonactive reaction using [$L_1ZnOEt]_0$ below the threshold value. Similar levels of deactivating impurity also have been observed for several other reported LA polymerization catalysts.[4,5b] With **2a**, when special care was taken to decrease the impurity level below the threshold found in the kinetic experiments, use of high [LA]$_0$/[$L_1ZnOEt]_0$ ratios led successfully to very high molecular weight PLA (up to 130 kg mol$^{-1}$). An alternative analysis of the rate data using plots of ln($k_{obs}$) versus ln([$L_1ZnOEt]_0$) yielded nonintegral orders in catalyst (Figure 7a), similar to previous reports that invoked aggregation phenomena as a rationale.[9,30] On the basis of the combined experimental data, we deem this interpretation less likely to be correct in our system. Indeed, we caution against only evaluating order in catalyst using the logarithmic analysis because the possibility of a deactivating impurity is effectively obscured if the nonintegral order is accepted without further scrutiny.

The coordination−insertion pathway shown in Scheme 2 is consistent with the second order rate law and with the analysis of polymer end groups. Additional chain exchange processes also are illustrated, which are postulated in order to explain the lower than predicted polymer molecular weights that we measured accurately using SEC with light scattering detection. Fits to the data in the plots of $M_n$ versus % conversion and ([LA]$_0$ − [LA]$_t$)/[$L_1ZnOEt]_0$ (Figures 5 and 6) enabled [$L_1$-$ZnOEt]_{eff}$ to be determined, but in the absence of definitive values for deactivating impurity concentration ([CD]), only a possible range for the concentration of the exchange agent ([EA]) could be calculated: ∼0.4 mM < [EA] < ∼1.3 mM. Although relatively low, these concentrations are significant at low catalyst loadings (high [LA]$_0$/[$L_1ZnOEt]_0$) and can considerably decrease the observed polymer molecular weight. In further support of the feasibility of chain exchange processes, we found that added BnOH lowered the polymer molecular weight without affecting the polymerization rate or polydisper-

sity. These results are consistent with BnOH being an effective chain exchange reagent and with exchange being more rapid than monomer enchainment.[26]

The observed effects of CD and EA on the polymerization kinetics and polymer molecular weights may be rationalized by invoking water as an adventitious impurity that reacts with **2a** according to eq 5, assuming that $L_1ZnOH$ (or an oligomerized form) is capable of rapid chain exchange but is inactive for chain propagation. According to this hypothesis, substoichiometric water decreases the amount of active catalyst ($L_1ZnOR$) yet produces twice the amount of chain exchange reagents ($L_1ZnOH$ and EtOH) compared to the amount of catalyst deactivated. An alternative scenario suggested by a reviewer may also be envisioned wherein water acts to hydrolyze LA to lactic acid, which exchanges with the more basic phenolate ligand to yield an inactive carboxylate/alkoxide species. Decomposition of this species would liberate 2 equiv of chain exchange agent for each catalyst molecule deactivated. We recognize that although eq 5 or the above alternative adequately explains the experimental results, we lack conclusive data with which to unambiguously identify the nature of the trace reagents CD and EA.

$$2L_1ZnOEt + H_2O \rightarrow L_1ZnOEt + L_1ZnOH + EtOH \quad (5)$$

The remarkably rapid rate of LA polymerization by **2a** is worthy of note. Comparisons of $k_{obs}$ values at identical catalyst concentrations were used to rank **2a** within the set of most efficient LA polymerization catalysts for which kinetic data are available (Table 4), placing **2a** faster than other Zn(II)-containing catalysts. More insight is possible through comparison of propagation rate constants measured under identical conditions for reactions with identical rate laws. This is possible for **2a** and its dinuclear counterpart $LZn_2(Cl)_2OEt$,[4] for which $k_{prop}$ (0.37 $M^{-1}$ $s^{-1}$) is almost 6 times smaller at 25 °C in $CH_2Cl_2$. We speculate that the possible rate enhancing effect of the nearby Zn(II) in the dinuclear catalyst is inhibited by the chloride ligands, which yield metal sites with decreased Lewis acidity and a higher coordination number (CN = 4, not including the alkoxide) than those in "$L_1Zn$" (CN = 3). The ring opening polymerization activity of ($\beta$-diketiminate)Zn(II)-alkoxide catalysts has also been observed to correlate with the tendency to dimerize; bulkier ligands that favor the lower coordination number monomeric form induce greater polymerization activity.[31] Finally, we note that the very fast rate of LA polymerization by **2a** is a potentially quite useful characteristic, as it indicates a degree of kinetic lability that should enable ring opening polymerization of less reactive (i.e., low ring strain) monomers at low temperatures to generate new types of useful materials (e.g., perfectly alternating copolymers of hydroxy acids and epoxides).[32]

## Experimental Section

**General Methods and Materials.** All reactions were performed under a nitrogen atmosphere, using either standard Schlenk techniques

(31) Rieth, L. R.; Moore, D. R.; Lobkovsky, E. B.; Coates, G. W. *J. Am. Chem. Soc.* **2002**, *124*, 15239.
(32) Bechtold, K.; Hillmyer, M. A.; Tolman, W. B. *Macromolecules* **2001**, *34*, 8641.

or a glovebox. All solvents and reagents were obtained from commercial sources and used as received unless otherwise stated. Pentane, dichloromethane, and toluene were passed through purification columns (Glass Contour, Laguna, CA). Deuterated solvents were dried over calcium hydride, distilled under vacuum, and stored under nitrogen. Ethanol and benzyl alcohol were distilled from calcium hydride. Diethyl zinc (1 M in hexanes) was distilled immediately prior to use. D,L-Lactide and L-lactide were purified by recrystallization from toluene, followed by repeated (2−3×) vacuum sublimation. NMR Spectra were collected on a Varian INOVA-300 or Varian INOVA-500 spectrometer. Elemental analyses were determined by Atlantic Microlab, Inc., Norcross, GA and Robertson Microlit Laboratories, Inc., Madison, NJ. The molecular weights and molecular weight distributions of the high molecular weight polymers were determined by size exclusion chromotography (SEC) in THF. Separation was achieved by three Phenomenex Phenogel columns with pore sizes of $10^3$, $10^4$, and $10^5$ Å. An interferometric refractometer (Wyatt Technology OPTILAB) and a multiangle light scattering detector equipped with a 632.8 nm laser (Wyatt Technology DAWN) positioned downstream of the columns enabled the determination of polymer molecular weights based on a d$n$/d$c$ value of 0.0576 mL $g^{-1}$. High resolution electrospray mass spectra were recorded on a Bruker Reflex III system. Direct laser desorption mass spectrometry was performed using a Bruker Reflex III MALDI-TOF mass spectrometer (Bruker Daltonics, Billerica, MA). Samples were spotted onto a stainless steel target in a glovebox and transported to the instrument in a sealed container. The plate was quickly taken from the container and inserted into the vacuum lock of the instrument. Exposure to air in each case was <10 s. The laser employed was a pulsed nitrogen laser operating at 337 nm with a maximum average power of 6 mW. Typically, the laser power was attenuated by 10−20 dB in order to obtain satisfactory spectra for the samples analyzed. The instrument was operated in reflectron mode using delayed extraction techniques to improve resolution. The ^{1}H PGSE experiments were performed on a Varian INOVA 600 MHz spectrometer equipped with a triple axis gradient unit and a BioSelect HCN triple axis probe with actively shielded gradients. Samples were prepared by dissolving 5 mg of **1a**, **2a**, or **3** in 0.4 mL of $CD_2Cl_2$, and data were collected at 298 K without spinning the sample. A published pulse sequence was used to suppress convection artifacts[33] with a gradient length of 4 ms and a diffusion time of 30 s. The data were analyzed as described in the text.

**2,4-Di-*tert*-butyl-6-{[(2′-dimethylaminoethyl)methylamino]methyl}-phenol (HL₁).** *N,N,N′*-Trimethylethylenediamine (7.90 g, 75.0 mmol), *para*-formaldehyde (3.08 g, 97.5 mmol), and 2,4-di-*tert*-butylphenol (15.63 g, 75.0 mmol) were dissolved in ethanol (50 mL). The solution was heated at reflux for 14 h under nitrogen and then cooled to room temperature. Hydrobromic acid (12.73 mL, 112.5 mmol, 48% solution) was then added, and the liquid solution began to gel. This gel was dried thoroughly under vacuum to yield a solid, which was washed with ethanol to remove all of the yellow color. The white solid was dissolved in water (300 mL), neutralized with NaHCO₃, and extracted into CHCl₃ (3 × 100 mL). The combined organic layers were dried, and the solvent was removed in vacuo to give a colorless oil (18.26 g, 56.97 mmol, 76%). ¹H NMR (CDCl₃, 300 MHz) δ 7.21 (1H, d, $^4J_{H-H}$ = 2.7 Hz, Ar$H$), 6.83 (1H, d, $^4J_{H-H}$ = 2.4 Hz, Ar$H$), 3.69 (2H, s, NC$H_2$-Ar), 2.54 (4H, m, NC$H_2CH_2$N), 2.33 (3H, s, NC$H_3$), 2.23 (6H, s, N(C$H_3$)₂), 1.42 (9H, s, C(C$H_3$)₃), 1.29 (9H, s, C(C$H_3$)₃) ppm; ¹³C {¹H} NMR (CDCl₃, 75 MHz) δ 154.26, 140.15, 135.36, 123.33, 122.69, 121.28, 62.03, 57.00, 54.21, 45.68, 41.80, 34.78, 34.03, 31.67, 29.55 ppm. Anal. Calcd for $C_{20}H_{36}N_2O$: C, 74.95%; H, 11.32%; N, 8.74%. Found: C, 74.25%; H, 11.07%; N, 8.44%.

**2-*tert*-Butyl-4-methyl-6-{[(2′-dimethylaminoethyl)methylamino]-methyl}phenol (HL₂).** *N,N,N′*-Trimethylethylenediamine (3.10 g, 30.5 mmol), *para*-formaldehyde (1.20 g, 39.5 mmol), and 2-*tert*-butyl-4-methylphenol (5.00 g, 30.5 mmol) were dissolved in ethanol (25 mL).

(33) Jerschow, A.; Müller, N. *J. Magn. Reson.* **1997**, *125*, 372.

The solution was heated at reflux for 14 h under nitrogen and cooled to room temperature. Hydrobromic acid (5.00 mL, 45.8 mmol, 48% solution) was then added, and the liquid solution began to gel. This gel was dried thoroughly under vacuum to yield a solid, which was washed with ethanol to remove all of the yellow color. The white solid was dissolved in water (300 mL) and extracted with $CH_2Cl_2$ (3 × 100 mL). The aqueous layer was neutralized with $NaHCO_3$ and further extracted into $CH_2Cl_2$ (3 × 100 mL). The combined organic layers were dried over $Na_2SO_4$, and the solvent was removed in vacuo to give a colorless oil (7.50 g, 23.2 mmol, 76%). $^1H$ NMR ($CDCl_3$, 300 MHz) $\delta$ 6.95 (1H, s, Ar*H*), 6.62 (1H, s, Ar*H*), 3.62 (2H, s, NC*H₂*Ar), 2.51 (4H, m, NC*H₂CH₂*N), 2.29 (3H, s, NC*H₃*), 2.21 (3H, s, NC*H₃*), 2.11 (3H, s, NC*H₃*), 1.38 (9H, s, C(C*H₃*)₃) ppm; $^{13}C$ {$^1H$} NMR ($CDCl_3$, 75 MHz) $\delta$ 154.43, 136.01, 127.19, 126.42, 122.08, 61.51, 56.96, 54.10, 53.35, 45.54, 41.60, 34.48, 29.52, 20.72 ppm. HRMS calcd for $C_{17}H_{30}N_2O_1$ ($M^+ + 1$) 279.2358, found 279.2409.

**L₁ZnEt (1a).** $HL_1$ (2.00 g, 6.24 mmol) was dissolved in pentane (5 mL), and the solution was cooled to −35 °C. Diethyl zinc (6.24 mL of a 1 M solution in hexane, 6.24 mmol) was added to this solution slowly, and the mixture was stirred overnight at room temperature. The resulting precipitate was collected by filtration, washed with cold pentane (2 × 10 mL), and dried in vacuo (1.64 g, 3.96 mmol, 63%). Crystals suitable for X-ray crystallographic analysis were grown from pentane (−35 °C). $^1H$ NMR ($CD_2Cl_2$, 300 MHz) $\delta$ 7.16 (1H, d, $^4J_{H-H}$ = 2.7 Hz, Ar*H*), 6.78 (1H, d, $^4J_{H-H}$ = 2.4 Hz, Ar*H*), 3.66 (1H, d, $^2J_{H-H}$ = 12 Hz, NC*H₂*C), 3.43 (1H, d, $^2J_{H-H}$ = 12 Hz, NC*H₂*C), 2.62 (4H, m, NC*H₂CH₂*N), 2.50 (3H, s, NC*H₃*), 2.37 (3H, s, NC*H₃*), 2.08 (3H, s, NC*H₃*), 1.41 (9H, s, C(C*H₃*)₃), 1.25 (9H, s, C(C*H₃*)₃), 1.22 (3H, t, $^3J_{H-H}$ =8.1 Hz, CH₂C*H₃*), 0.04 (2H, q, $^3J_{H-H}$ =8.1 Hz, C*H₂*CH₃) ppm; $^{13}C$ {$^1H$} NMR ($CD_2Cl_2$, 75 MHz) $\delta$ 165.06, 137.80, 134.93, 126.27, 124.36, 122.74, 62.56, 57.96, 52.98, 47.78, 46.10, 45.97, 35.69, 34.24, 32.20, 30.05, 13.64, 4.00 ppm. Anal. Calcd for $C_{22}H_{40}N_2OZn$: C, 63.83%; H, 9.74%; N, 6.77%. Found C, 63.50%; H, 9.59%; N, 6.71%.

**L₂ZnEt (1b).** $HL_2$ (2.00 g, 6.24 mmol) was dissolved in pentane (10 mL), and the solution was cooled to −35 °C. Diethyl zinc (7.10 mL of a 0.88 M solution in hexane, 6.24 mmol) was added to this solution slowly, and the mixture was stirred overnight at room temperature. The resulting precipitate was collected by filtration, washed with cold pentane (2 × 10 mL), and dried in vacuo (1.51 g, 4.06 mmol, 65%). $^1H$ NMR ($CD_2Cl_2$, 300 MHz) $\delta$ 6.94 (1H, d, $^4J_{H-H}$ = 4.0 Hz, Ar*H*), 6.61 (1H, d, $^4J_{H-H}$ = 3.5 Hz, Ar*H*), 3.65 (1H, d, $^2J_{H-H}$ = 20.0 Hz, NC*H₂*C), 3.39 (1H, d, $^2J_{H-H}$ = 20.0 Hz, NC*H₂*C), 2.78 (4H, m, NC*H₂CH₂*N), 2.49 (3H, s, NC*H₃*), 2.37 (3H, s, ArC*H₃*), 2.17 (3H, s, NC*H₃*), 2.12 (3H, s, NC*H₃*), 1.40 (9H, s, C(C*H₃*)₃), 1.22 (3H, t, $^3J_{H-H}$ = 14.0 Hz, CH₂C*H₃*), 0.05 (2H, q, $^3J_{H-H}$ =8.1 Hz, C*H₂*CH₃) ppm; $^{13}C$ {$^1H$} NMR ($CD_2Cl_2$, 75 MHz) $\delta$ 165.16, 138.632, 130.08, 128.27, 121.08, 62.25, 57.99, 52.95, 47.77, 46.21, 45.95, 35.37, 30.05, 20.95, 13.61, −4.06 ppm. Anal. Calcd for $C_{19}H_{34}N_2OZn$: C, 61.35%; H, 9.21%; N, 7.56%. Found C, 59.90%; H, 8.90%; N, 7.31%.

**(L₁ZnOEt)₂ (2a).** Complex **1a** (1.00 g, 2.42 mmol) was dissolved in toluene (13 mL) and cooled to −35 °C. Ethanol (0.14 mL, 2.42 mmol) was added to this solution slowly. The mixture was stirred for 1 d at room temperature and then filtered through Celite. The filtrate was dried in vacuo to give a white solid (0.85 g, 1.98 mmol, 82%). Crystals suitable for X-ray diffraction were grown from a mixture of toluene and pentane at −35 °C. $^1H$ NMR ($CD_2Cl_2$, 300 MHz, see Figure S1) $\delta$ 7.19 (1H, d, $^4J_{H-H}$ = 2.4 Hz, Ar*H*), 6.79 (1H, d, $^4J_{H-H}$ = 2.7 Hz, Ar*H*), 3.92 (2H, q, $^3J_{H-H}$ = 6.8 Hz, OC*H₂*CH₃), 3.80 (1H, d, $^2J_{H-H}$ = 10.2 Hz, NC*H₂*C), 3.53 (1H, d, $^2J_{H-H}$ = 12.0 Hz, NC*H₂*C), 2.76 (4H, m, NC*H₂CH₂*N), 2.55 (3H, s, NC*H₃*), 2.32 (6H, m, N(C*H₃*)₂), 1.43 (9H, s, C(C*H₃*)₃), 1.26 (9H, s, C(C*H₃*)₃), 1.21 (3H, t, $^3J_{H-H}$ = 6.8 Hz, OCH₂C*H₃*) ppm; $^{13}C$ {$^1H$} NMR ($CD_2Cl_2$, 75 MHz) $\delta$ 164.43, 138.13, 135.59, 126.48, 124.57, 121.63, 63.29, 62.36, 57.24, 52.98, 47.27, 45.17, 35.72, 34.25, 32.18, 30.07, 22.83 ppm. Anal. Calcd for $C_{22}H_{40}N_2O_2Zn$: C, 61.46%; H, 9.38%; N, 6.52%. Found C, 61.58%; H, 9.32%; N, 6.16%.

**(L₂ZnOEt)₂ (2b).** Complex **1b** (0.50 g, 1.34 mmol) was dissolved in toluene (10 mL) and cooled to −35 °C. Ethanol (0.14 mL, 2.42 mmol) was added to this solution slowly. The mixture was stirred for 12 h at room temperature and then filtered through Celite. The filtrate was dried in vacuo to give a white solid (0.47 g, 1.21 mmol, 90%). This compound was recrystallized from toluene and pentane at −35 °C prior to use in LDMS and NMR crossover experiments. $^1H$ NMR ($CD_2Cl_2$, 300 MHz) $\delta$ 6.96 ($^1/_2$H, d, $^4J_{H-H}$ = 4.0 Hz, Ar*H*), 6.93 ($^1/_2$H, d, $^4J_{H-H}$ = 4.0 Hz, Ar*H*), 6.61 (1H, d, $^4J_{H-H}$ = 3.0 Hz, Ar*H*), 3.88 (2H, q, $^3J_{H-H}$ = 12.0 Hz, OC*H₂*CH₃), 3.77 (1H, s, NC*H₂*Ar), 3.37 (1H, d, $^2J_{H-H}$ = 20.0 Hz, NC*H₂*Ar), 2.77 (4H, m, NC*H₂CH₂*N), 2.59 (3H, s, NC*H₃*), 2.22 (3H, s, C*H₃*Ar), 2.17 (6H, s, N(C*H₃*)₂), 1.40 (9H, s, C(C*H₃*)₃), 1.21 (3H, t, $^3J_{H-H}$ = 11.5 Hz, OCH₂C*H₃*) ppm; $^{13}C$ {$^1H$} NMR ($CD_2Cl_2$, 75 MHz) $\delta$ 164.09, 138.57, 130.01, 128.09, 121.28, 65.18, 57.07, 46.92, 45.18, 44.05, 35.41, 35.24, 29.99, 20.86 ppm. Anal. Calcd for $C_{19}H_{34}N_2O_2Zn$: C, 58.81%; H, 8.83%; N, 7.25%. Found C, 58.61%; H, 8.97%; N, 7.91%.

**Typical Polymerization Procedure.** All glassware used for polymerizations was oven dried, treated with a 1.0 M solution of $Me_2SiCl_2$ in $CH_2Cl_2$, and dried for a minimum of an additional 3 h at 200 °C. The solvent, $CH_2Cl_2$, was passed through a plug of alumina immediately prior to use. A stock solution of catalyst, **2a**, was prepared such that $[L_1ZnOEt]_0$ = 0.0023 M in $CH_2Cl_2$ and was stored under nitrogen at −35 °C. A representative procedure is given below. In the glovebox, a glass vial was charged with LA (0.180 g, 1.25 mmol, 1500 equiv) and $CH_2Cl_2$ (1.21 mL). A volume (0.036 mL, $8.32 \times 10^{-4}$ mmol, 1 equiv) of the catalyst stock solution was injected into the monomer solution and stirred at room temperature. After stirring for an appropriate time, an aliquot was withdrawn from the reaction and the product polymer was precipitated by adding excess (2 mL) pentane, followed by removal of the solvents in vacuo at RT.

**Kinetics.** Data for the polymerization of LA by **2a** were collected by an in situ monitoring of the changes in IR spectra using an ASI Applied Systems ReactIR 4000 spectrometer. For the 25 °C runs, a reaction flask was charged with LA and a solution of **2a** in $CH_2Cl_2$ in the glovebox (the total volume varied, but the average volume was approximately 3 mL). The ReactIR probe was then attached to the flask via a ground glass joint, and the apparatus was removed from the glovebox and attached to the IR spectrometer so that the reaction flask was immersed in a temperature controlled bath at 25 °C. For the 0 °C runs, catalyst was not added in the glovebox, and the apparatus was subsequently immersed in an ice−water bath. The solution temperature was allowed to equilibrate over 5 min, and **2a** (as a $CH_2Cl_2$ stock solution prepared in the glovebox) was injected through a septum via syringe. Peaks due to LA at 1345, 1240, and 930 $cm^{-1}$ and peaks due to PLA at 1184, 1147, 1131, and 863 $cm^{-1}$ were monitored; analysis of LA decay and PLA growth gave very similar results. The observed rate constants ($k_{obs}$) were extracted by fitting an exponential curve to the plot of absorbance versus time using $A_t = (A_0 - A_\infty)e^{-kt} + A_\infty$, allowing $A_0$, $A_t$, and $k$ to vary freely and taking the average value from the seven peaks monitored. The data were analyzed over at least four half-lives. All linear and nonlinear curve fits were performed with KaleidaGraph.

**X-ray Crystallography.** Single crystals of **1a** and **2a** were attached to glass fibers and mounted on a Siemens or Bruker SMART system for data collection at 173(2) K. An initial set of cell constants was calculated from three sets of 20 frames. These initial sets of frames were oriented such that orthogonal wedges of reciprocal space were surveyed; orientation matrixes were calculated from 90 to 150 reflections. The data collection was performed using Mo K$\alpha$ radiation with a frame time of 20 and 45 s, respectively, and a detector distance of 4.9 cm. A randomly oriented region of reciprocal space was surveyed to the extent of 1.5 hemispheres and to a resolution of 0.84 Å. Three major sections of frames were collected with 0.30° steps in $\omega$ at three different $\phi$ settings and a detector position of −28° in 2$\theta$. The intesity data were corrected for absorption and decay (SADABS).[34] Final cell

constants were calculated from the *xyz* centroids of strong reflections from the actual data collection after integration (SAINT).[35] The structures were solved by direct methods using SIR92[36] and SIR97,[37] which located most of the non-hydrogen atoms from the E-map. Full-matrix least squares/difference Fourier cycles were performed using SHELXL-97.[38] Space groups were determined based on systematic absences and intensity statistics. All non-hydrogen atoms were refined with anisotropic displacement parameters. All hydrogen atoms were placed in ideal positions and refined as riding atoms with relative isotropic displacement parameters. For **2a**, solvent molecules (toluene, pentane) were found in channels throughout the crystal and could not be individually modeled. To obtain a better model, the solvent molecules were removed using program PLATON, function SQUEEZE.[36] Full crystallographic information for each complex is available in its CIF.

**Supporting Information Available:** NMR spectrum of **2a** (Figure S1), representative kinetic trace (Figure S2), listing of $k_{obs}$ values (Table S1), and X-ray crystallographic data (CIF). This material is available free of charge via the Internet at http://pubs.acs.org.

JA0359512

(34) An empirical correction for absorption anisotropy. Blessing, R. *Acta Crystallogr.* **1995**, *A51*, 33.

(35) *SAINT V6.2*; Bruker Analytical X-ray Systems: Madison, WI, 2001.

(36) (a) Spek, A. L. *Acta Crystallogr.* **1990**, *A46*, C34. (b) Spek, A. L. *PLATON, A Multipurpose Crystallographic Tool*; Utrecht University: Utrecht, The Netherlands, 2000.

(37) Altomare, A.; Burla, M. C.; Camalli, M.; Cascarano, G.; Giacovazzo, C.; Guargliardi, A.; Moliterni, A. G. G.; Polidori, G.; Spagna, R. SIR97: a new tool for crystal structure determination and refinement. *J. Appl. Crystallogr.* **1998**, *32*, 115.

(38) *SHELXTL V6.10*; Bruker Analytical X-ray Systems: Madison, WI, 2000.